

# An MR-Compatible Device for Imaging the Lower Extremity during Movement and Under Load

*Client:*

Darryl Thelen

*Advisor:*

William Murphy

*Team Members:*

Sarajane Stevens

Arinne Lyman

Christopher Westphal

Eric Bader

## Table of Contents

Abstract.....	3
Problem Statement.....	4
Background Information .....	4
Current Devices .....	6
Design Constraints.....	8
Loading Systems.....	8
Alternate Designs.....	11
Design Matrix .....	13
Equations of Motion .....	14
Final Design.....	17
Materials and Cost.....	18
Manufacturing.....	19
Future Work.....	20
Ethics and Intellectual Property Issues .....	21
References.....	22
Appendix.....	24
Anthropometric Data .....	24
Equations and Values for Extreme Anthropometric Limits .....	25
Dimensions of Design.....	26
Product Design Specifications .....	28

## **Abstract**

Hamstring strain injuries are one of the most common muscle maladies in athletes, especially runners. Injury usually occurs late in swing phase when the hamstring is undergoing eccentric contraction to decelerate the limb. Re-injury is very common after recovery from these injuries, suggesting current clinical assessment tools may be insufficient to assess biomechanical function and re-injury risk before return to sport. Most current imaging techniques that are used to assess this function can only do so under static conditions, thus they cannot provide direct measurements of muscle properties and mechanical strain under dynamic loadings, such as seen in running. We have developed a device that will load the leg at a percentage of a subject's maximum voluntary contraction via inertia through extension of the knee. Most of the semester was spent conceptualizing and analyzing a system to simulate muscle loading during running within a MR magnet. To do this, we developed equations of motion that define our system and performed a free body analysis on our design to be sure that our inertial load was feasible for us to construct. The final prototype consists of the subject lying prone on the base of the device with the ankle attached to a plastic chain that turns three sprockets. The other end of the chain is connected to the counterweight that supports the weight of the shank and for each turn of the sprockets, the disks provide a rotational inertial load to the hamstring during extension. This device will be tested in the motion lab over the next few weeks to measure the movement of the shank and test the repeatability of the motion. Subsequently, the device will be used in conjunction with CINE-Phase Contrast MRI to measure muscle velocity of the hamstring muscles undergoing eccentric contractions. Any further modifications to the prototype will be determined after testing is complete.

## **Problem Statement**

MR imaging can provide clinicians and researchers valuable insights into the morphology of musculoskeletal structures. However, most current imaging techniques in use are static and don't provide direct measurements of biomechanical function. Recent breakthroughs in magnet strength, acquisition speed and processing of MR data have enabled imaging to be used to measure in-vivo muscle motion and joint kinematics during movement. These applications require the use of a non-magnetic device for loading or guiding the limb through a desired, repeatable movement. The goal of this design project is to develop and build such a device for use in the Radiology clinic at the University of Wisconsin Hospital. Our initial intended applications are to use Cine-PC (Phase contrast) imaging to measure in-vivo musculotendon motion of the hamstrings muscles during a stretch-shortening cycle. Cine-PC requires multiple cycles of motion, necessitating that the device guide the limb through a repeatable motion at relatively low loads.

## **Background Information**

The gait cycle is comprised of the movements of the leg and foot during running or walking. A full cycle consists of a stance phase and swing phase where the foot is touching the ground and in the air respectively. For running, the gait cycle is modeled in Figure 1 [10]. Swing phase is the part of the gait cycle of most interest to clinicians studying muscle injuries. It is during this phase that the muscle must rapidly change direction of the leg in order to contact the ground in front of the runner. Because of the inertial load applied to the leg muscles is so large due to the weight of the shank, the muscles can be subject to tear or injury when the swing leg becomes fully extended.

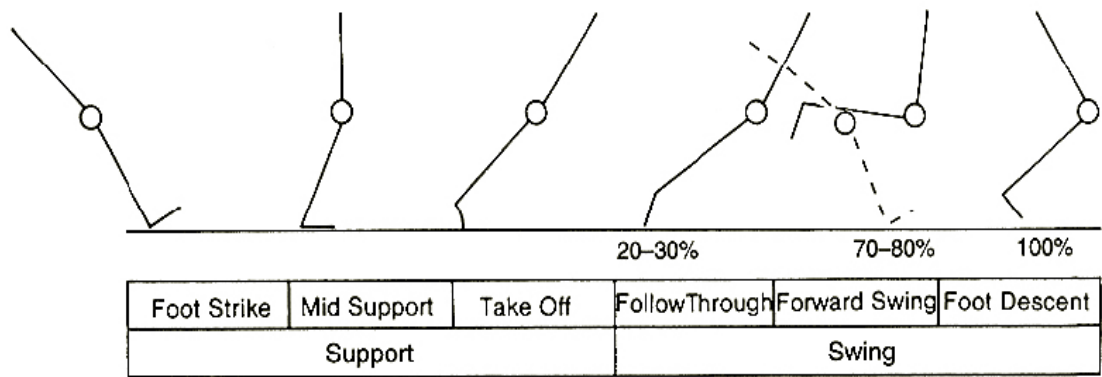


**Figure 1: Running Gait Cycle.** Shown above are the different phases of the gait cycle while running. [10]

In athletics, the hamstring muscle is one of the most frequently strained muscles during high speed running [20]. A large number of these strains involve the biceps femoris, the most lateral muscle of the group of three biarticular muscles comprising the hamstrings (Figure 2).

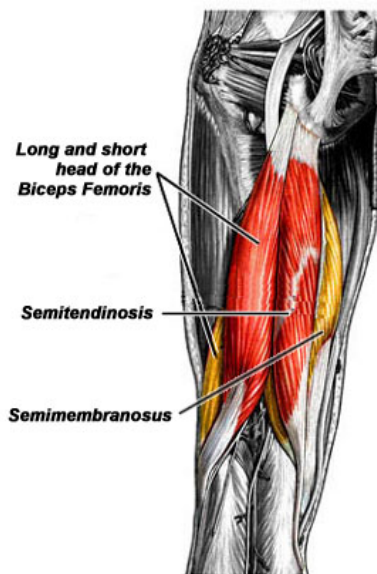


**Figure 2: Gross Anatomy of Hamstring Group.** Three muscles comprise the hamstring: biceps femoris, semitendionosus, semimembranosus. [21]

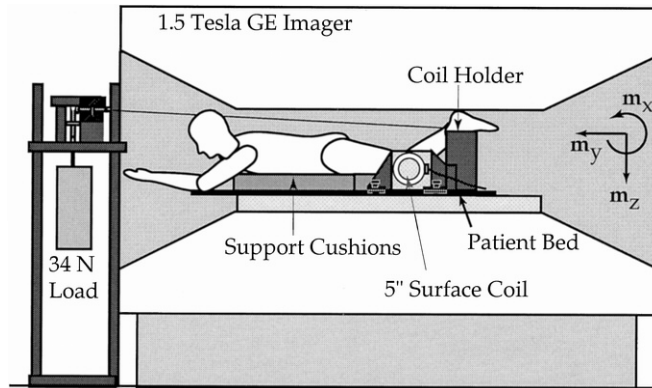
A strain results when the muscle fibers are torn at the musculotendon junction. Such injuries commonly occur as a result of an eccentric contraction performed by a stretched muscle under load. It has been suggested that late swing phase before heel strike is a main cause of this injury due to the hamstring muscles being active and

lengthening at this phase, which induces eccentric contraction [20]. Appropriate treatment of acute muscle strain injuries remains debated, and can range from stretching to total immobilization. Furthermore, little is known about how specific rehabilitation programs or previous hamstring injury affects biomechanical function of the muscle upon return to sport. Thus, the objective of this project is to design a device that will create a physiological load on the hamstring during a stretch-shortening cycle. Muscle velocity will then be assessed using phase contrast imaging, integrated to estimate displacements and strains, and then compared to the contralateral leg to determine differences in spatial strain distributions.

### **Current Devices**

Initial literature and patent research was conducted on existing load-bearing MRI devices. A total of twelve devices were found in literature to load the biceps brachii, rectus femoris, and biceps femoris. Some of the major differences between the devices were passivity, imaging sequences used, degrees of flexion, position of the subject, and type of loading. For example, Sheehan *et al.* had their subjects lie in a prone position inside the MRI bore and extend their knees at a rate of 35 cycles per minute against a 34N load/pulley system as shown in Figure 3. They used a metronome (auditory signal) to ensure repeatability of motion and simulated walking using this motion. Limitations to this device include a constant load on all subjects regardless of body mass or strength, the creation of an extensor torque on the knee, and motion artifact due to the unknown accuracy of fast-PC imaging [18,19].

**Figure 3:** *Experimental setup.* Subject in prone position extending leg against 34N load. [18,19]



Another device is by Patel *et al.* consisted of a PVC pipe apparatus attached to a weight/pulley system. Subjects were asked to lay supine and standing was simulated by a constant force application of 13.61kg through a footplate as shown in Figure 4. Five different knee flexion positions were imaged to determine axial loading on the knees during stance. Limitations to this device are the fatigue of the patient and the additional gravitational load experienced by the knee. The loading was not physiologically comparable to standing because of patient fatigue [13,14,15].



**Figure 4:** *Weight Bearing Apparatus.* Subject lies supine flexing against a constant weight of 133N. [14]

None of the devices found in literature loaded the hamstring during leg extension as during swing phase of running or sprinting. Also, all of the devices relied on either passive motion or patient reliability using a metronome when constraining the endpoints. We would like to come up with a more accurate way of having a repeatable, harmonic cycle while also generating a physiological load on the hamstring.

## **Design Constraints**

Since none of the current devices in literature fit the needs of our client, we must design our own device that will cause the hamstring to undergo a stretch-shortening cycle under a constant or variable load. Our device must control the force level the patient feels and control this force throughout the cycle within  $\pm 5\%$ . The force must be a physiological force that is usually applied during running, but can be a percentage of the person's maximum voluntary contraction so as not to allow fatigue during many repetitions. It cannot allow any lateral movement of the leg as it will induce non-sagittal movement of the muscle, which is imaged in a single plane. Additionally, we would like to counteract the weight of gravity by using a counterweight. Since the weight of the shank might exceed 15% of the subject's maximum voluntary contraction, he/she may fatigue when doing repeated cycles of the same motion [12]. Ideally we want to simulate swing phase of running or sprinting, but the range of motion of the shank is limited due to the small size of the MRI bore. The periodic movement of the leg must be repeated within  $\pm 1$  degree at each endpoint and  $\pm 3$  degrees at any other place in the cycle. The device should support the thigh and allow the shank to move freely. The device should be as light as possible to allow for transport to and from the imaging room in the hospital. It cannot contain any metallic or ferrous materials due to the magnetic field strength of the MRI. A complete product design specification report is included in the Appendix.

## **Loading Designs**

There are many different ways to load muscles in the leg including using gravitational loads (resistance training), spring system, damper system, or an inertial system. A gravitational loading system can consist of pushing against a set of weights as

in leg press machines, however when performed slowly this applies a constant force to the muscles which does not represent physiological loads during running (Figure 5). We would like the hamstring to have maximum torque near the end of swing phase which occurs during the last 20% of the gait cycle [20].

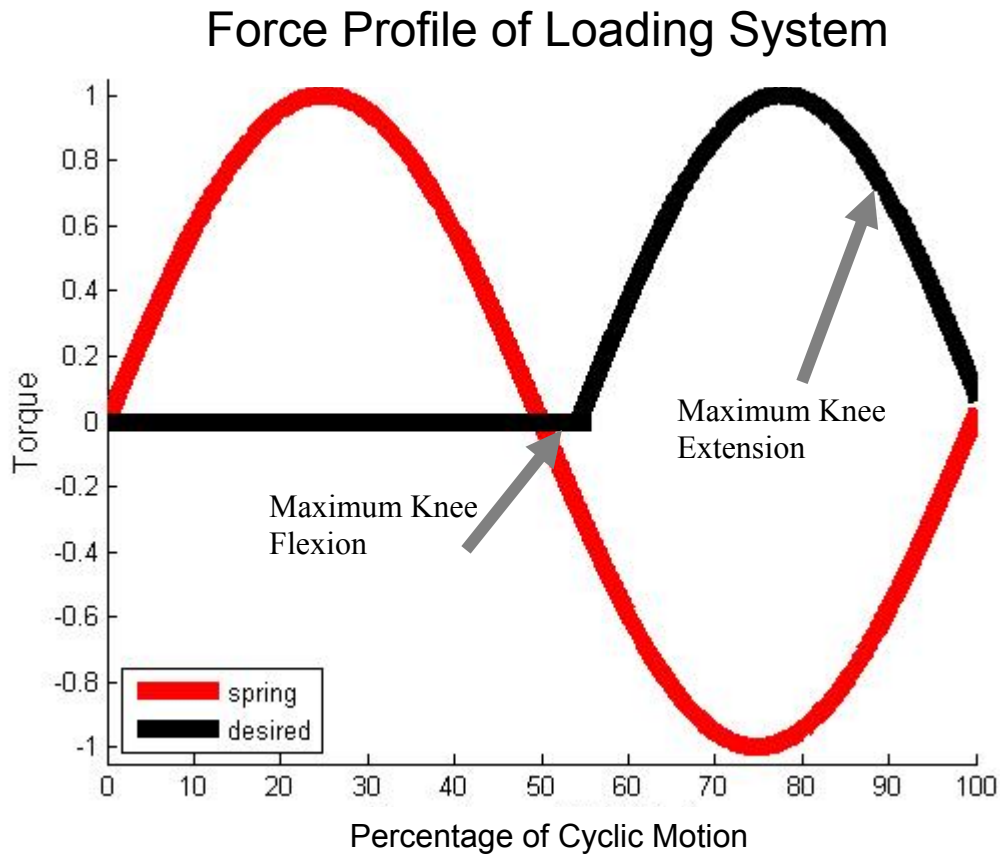


**Figure 5:** *Force Profile of Spring and Desired Loading.* In comparison of the desired force curve, the spring is out of phase by 180 degrees.

A damper system applies a load as a function of velocity, thus its loading system is the derivative of the spring system, which is a function of position. The damper force profile is shown in Figure 6. It is able to accomplish loading of the hamstring during the last part of the gait cycle, but also loads the muscle early and creates a negative torque on the muscle during the middle of the cycle. This is not a physiological load as the hamstring is not active during mid-swing phase.

## Force Profile of Loading System

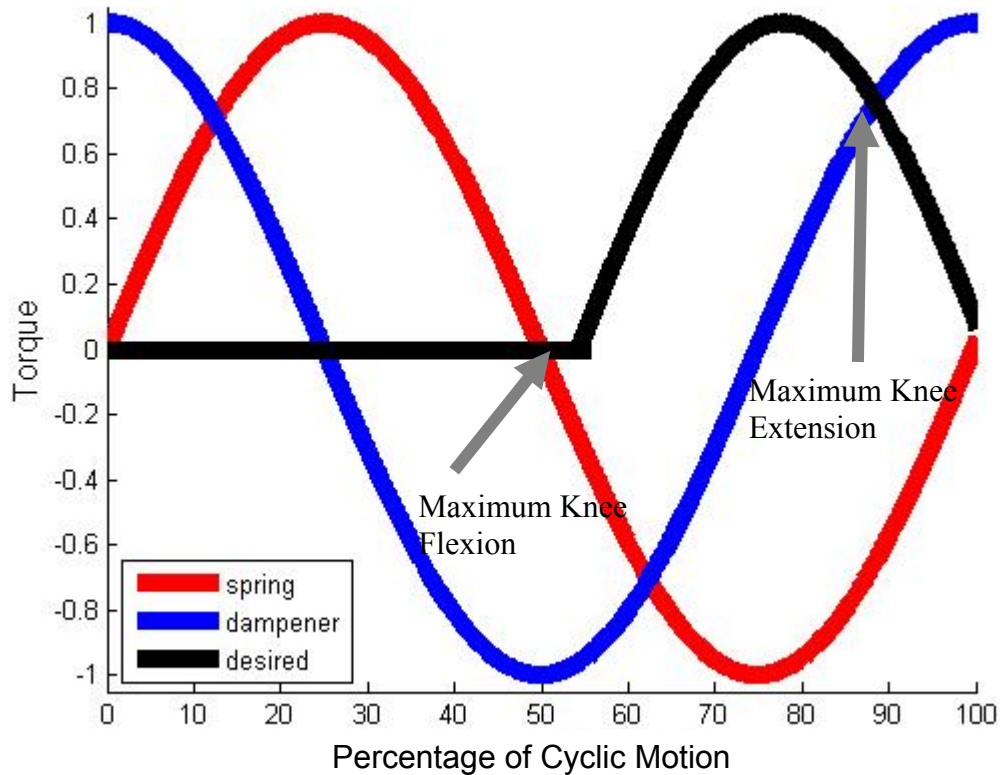


**Figure 6:** *Force Profile of a Spring, Damper, and Desired Loading.* Placing a damper in this system would allow a torque to be generated near our desired time, but would not be optimal.

For our last loading design, we thought inertia would be best to create a force on the hamstring since inertial forces are responsible for much of the hamstring loading seen during the late swing phase running. Inertia is a function of acceleration which is the derivative of the velocity profile. This will provide maximum load on the hamstrings when the knee is extended, akin to running (Figure 7). In addition, we can tailor the inertial model to fit any individual by adjusting the amount of inertia applied to the system.

## Force Profile of Loading System

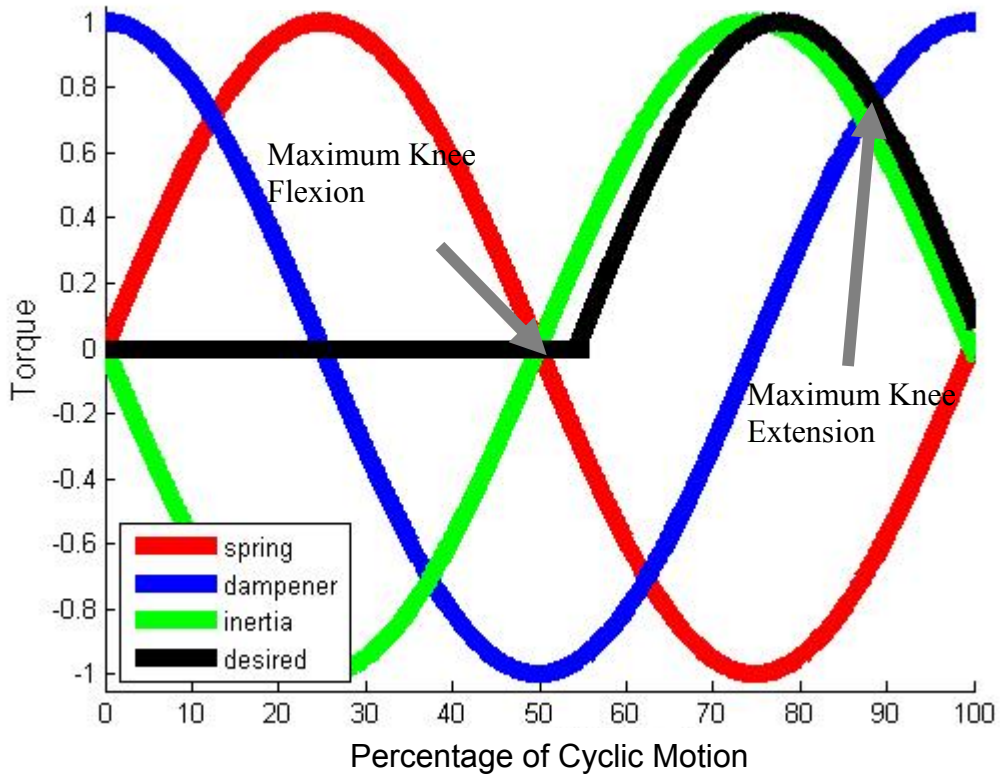


**Figure7:** *Force Profile of a Spring, Damper, Inertia, and Desired Loading.* Using an inertial component in our design will provide the best representation of a physiological load.

### Alternate Designs

Two main designs were created regarding the position of the subject with respect to the MRI table. The first has the subject lying prone on the table with the legs moving in the vertical plane, while the second design has the subject on their side in a lateral position with the leg moving horizontally. An advantage to the prone position is that the subject can lie comfortably on the table and move the leg with little restriction aside from the bore height. A simple open loop design may be used in this position. Gravity acts on the leg because it is moving in the vertical plane, thus the leg must be counterbalanced in order to negate the effects of gravity.

The lateral position does not need to account for gravity and the lower shank moves back and forth in order to maximize the range. The rotation of the shank on the MRI table could create static electricity causing image artifacts. This design also necessitates a closed loop design in order to ensure that the tension on the chain is constant, thus translating the motion from the limb to the load and vice versa.

If a simple open loop layout is to be used, there are two variations: the chain may exit out the back of the MRI and rest on the “doghouse” or the chain can run along the top of the bore and exit out the front while resting on the MRI bed. The front exit design provides visual feedback to the subject, but the long distance the chain must travel should be considered in the cost and stability of the design. If the load were to exit out the back, the chain would be shorter, but no visual feedback would be available and uncertainties regarding the space available are also an issue.

In all designs, there must be some ankle support to which the chain must be attached. This may be as simple as a lace-up ankle support commonly used for sprains in athletes. The thigh must also be constrained in order to reduce non-sagittal motion artifact.

The action of this device consists of active movement of the shank by the subject. The chain attached to the ankle will travel along multiple sprockets which are turning with the help of ball bearings to reduce friction. One sprocket will be attached to a rod holding various size disks with various inertia ratings. These can be mixed and matched according to the needs of the subject. The angular acceleration of the disks provides the inertia as the shank reaches each endpoint and must switch directions. The other end of

the chain which is not attached to the ankle will be attached to a counterweight for the shank.

### **Design Matrix**

Our various designs were ranked according to comfort, cost, accessibility, portability, feedback and manufacturing. Specific design constraints are not included in the design matrix because all designs satisfy the original client requirements. The scores were weighted to categories that were more important to the client. Comfort and visual feedback of the counterweight are important to the subject participating in the research. The motion should be as repeatable as possible—this may be altered by fatigue of the subject. Accessibility, portability and cost are also important to the client. Accessibility is crucial to setting up the device as it was designed. Portability has been considered because of the lack of storage space available, thus requiring it to be transported from the office to the hospital. Finally, cost is always a factor, especially in research where grant money is hard to receive. As seen in Table 1, the prone position with the chain exiting out the front of the bore is the preferred choice.

**Table 1:** *Design Matrix*

	<u>Prone</u>		<u>Lateral</u>
	Exit Back	Exit Front	
Comfort (10)	8	9	5
Cost (10)	8	6	3
Accessibility (8)	6	8	2
Portability (10)	7	6	3
Feedback (2)	0	2	0
Manufacturing (5)	4	4	2
<b>Total (45)</b>	<b>33</b>	<b>35</b>	<b>15</b>

Both of the prone designs provide similar comfort to the subject and ease of portability. However, the costs of the designs vary because of the amount of material required to make the design work (i.e. length of chain and bulk of inertia system assembly). When the chain exits the front, it allows the subject to turn their head and view the counterweight dropping.

### Equations of Motion

In order to confirm that our design would provide the right amount of inertia to the hamstring, we developed a simplified free-body diagram of the mechanism counterbalancing the shank and providing the inertia. This diagram is shown in Figure 8 and contains all relevant forces and velocities.

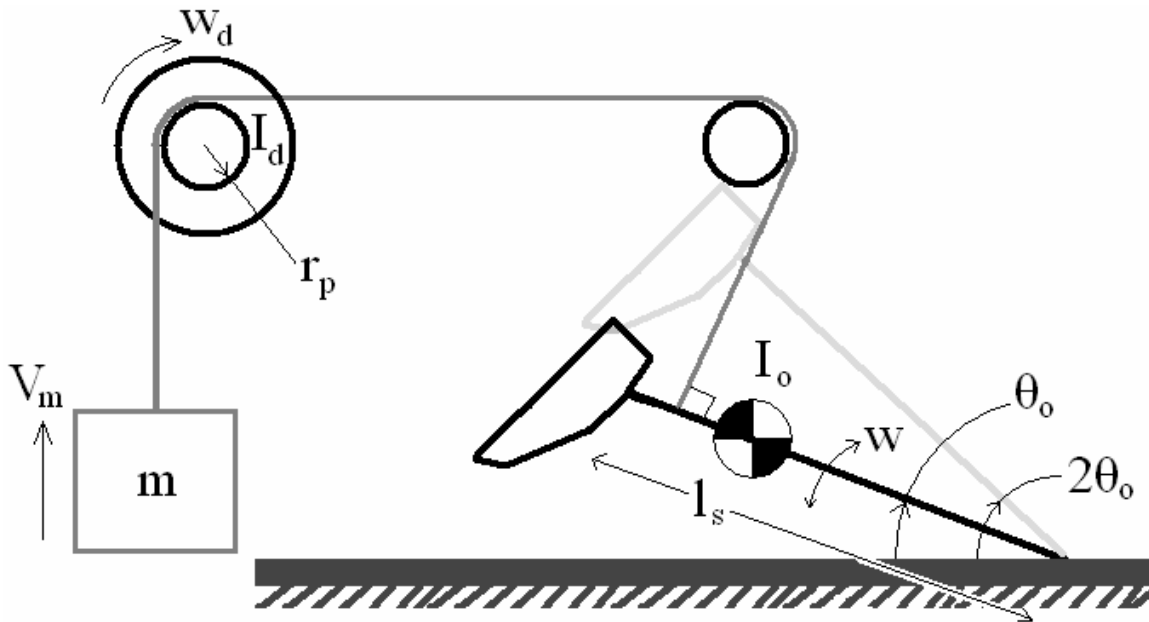


**Figure 8: Free Body Diagram.** The leg with length,  $l_s$ , and moment of inertia,  $I_o$ , moves at an angular velocity,  $w$ , through  $2\theta_o$  degrees. This movement rotates a sprocket with a radius of  $r_p$ , which in turn rotates the inertial disks. These disks have an inertia of  $I_d$  and rotate at an angular velocity of  $w_d$ . This movement also translates movement of a counterweight,  $m$ , at a velocity,  $V_m$ .

We were able to conceptualize our design to have one degree of freedom. We determined the equivalent inertia,  $I_e$ , of the system that would replicate the total kinetic

energy of the actual system, assuming that at half the maximum angle of the shank, the chain connected to the ankle was perpendicular to the shank. The equivalent free-body diagram is found in Figure 9.

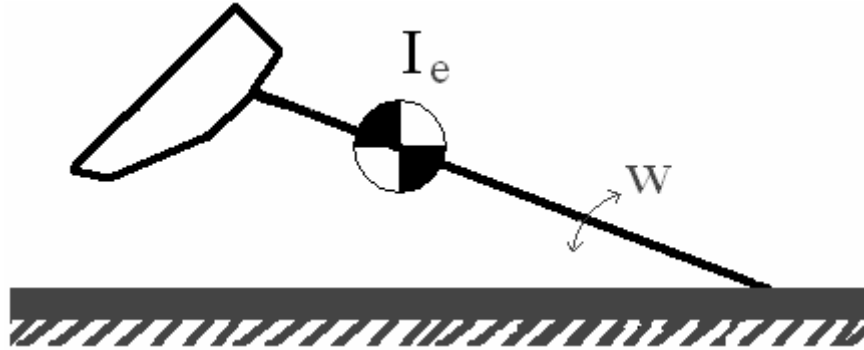


**Figure 9:** *Equivalent Free Body Diagram.* The variables from the free body diagram in Figure 8 can be condensed into an equivalent inertia,  $I_e$ , for the entire system rotating at an angular velocity,  $w$ .

To find our equations of motion, we determined the angular frequency  $\omega (=2\pi f)$ . The desired frequency would typically be 30 cycles/min, making one repetition done in two seconds. The angular position, angular velocity and acceleration are then given by:

$$\begin{aligned}\theta &= \theta_o + \theta_o \sin \omega t \\ \dot{\theta} &= \theta_o \omega \cos \omega t \\ \ddot{\theta} &= -\theta_o \omega^2 \sin \omega t\end{aligned}$$

We then equated the kinetic energy of our actual and idealized systems to determine the equivalent mass moment of inertia ( $I_e$ ).

$$\frac{1}{2}mv^2 + \frac{1}{2}I_d\omega_d^2 + \frac{1}{2}I_o\omega^2 = \frac{1}{2}I_e\omega^2$$

In order to prevent fatigue of the subject we were given a 100-250Nm torque constraint on the knee as determined by earlier maximum voluntary contraction data on the subjects involved in our client's study. Our value for torque due to the equivalent inertia must stay within 5-20% of the average value of maximum torque. Therefore:

$$5Nm < T < 50Nm$$

$$\left( ml_s + \frac{I_d l_s}{r_p^2} \right) < \frac{mg}{\dot{\omega}_{\max}}$$

From these inequalities, torque due to the equivalent inertia must be less than the weight of the shank or the chain will become slack.

We now have a range for the torque that can be applied to the knee as a function of the subject's maximum voluntary contraction, which will be determined in the lab before testing begins. Next, a free-body diagram of the counterweight and the inertia/pulley system was evaluated. The tension in the chain connecting the counterweight to the inertial load, represented as  $T_1$ , and connecting the shank to the inertial load, represented as  $T_2$ , was found to be

$$T_1 = mg + m\dot{v}$$

$$T_2 = T_1 + \frac{I_d}{r_p} \dot{\omega}_d$$

both of which need to be less than the weight of the counterweight or the chain would go slack. From these constraints, we were able to choose our final variables for determining the inertial load.

We decided to find the inertial load for the smallest, lightest female sprinter and the tallest, heaviest male football player. We chose heights of 1.499m and 1.905m and masses of 40kg and 115kg respectively. Using the anthropometric data contained in Appendix, we calculated the mass of the shank and foot, radius to center of mass of the shank and foot, radius of gyration of the shank and foot, and moment of inertia of the shank and foot for both subjects. These values can be found in a spreadsheet included in the Appendix.

We found the total moment of inertia of the shank plus the foot using the Parallel Axis Theorem and set that equal to the inertia of the shank ( $I_o$ ). We calculated the equivalent inertia for each individual using the theoretical torque due to maximum voluntary contraction and angular acceleration. Angular acceleration was calculated using the equations of motion and arc length due to the subject's shank length ( $l_s$ ).

Using the kinematic constraints ( $v = \omega * r$ ), we solved our conservation of energy for ( $I_d$ ) to determine the loading needed to cause the equivalent inertia on the leg. After substituting these values into our conservation of energy equation, we were able to choose values for disk radius ( $r_d$ ) and sprocket radius ( $r_p$ ) to solve for the mass of the inertial disks. We chose two inches for the disk and one inch for the sprocket and found that our design was feasible to manufacture in the machine shop.

### **Final Design**

Our final design consisted of two main components; the platform on which the subject lies, and the inertia system assembly. The platform consists of a guide rail, which supports a post that houses a sprocket (Figure 10). This sprocket guides the chain attached to foot, along the top of the MRI bore to the inertial system. In order to reduce friction of the system, each sprocket is fitted with a ball-bearing.

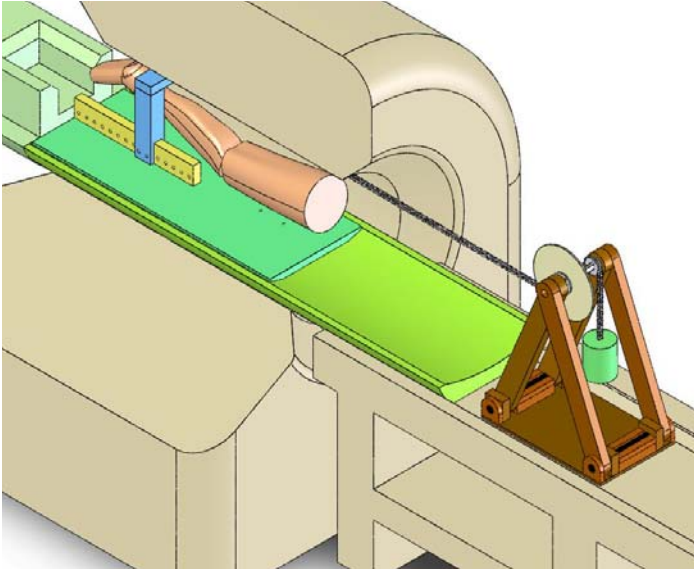


**Figure 10:** *Platform and Inertial System.* The subject lies prone in the MRI bore, extending the leg under inertial load.

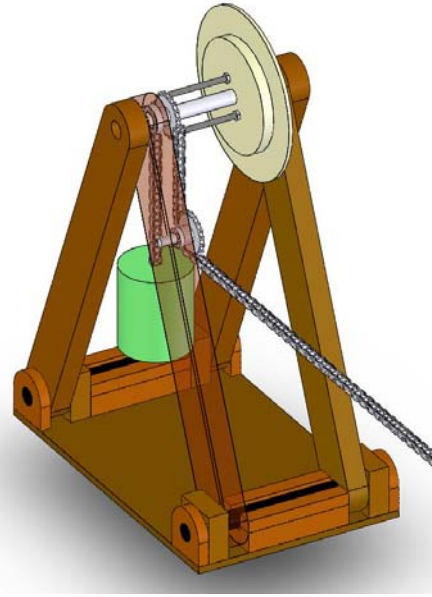


**Figure 11:** *Inertial Loading Assembly.* This is placed by the subject's head and is comprised of inertial disks and a counterweight.

The inertial system assembly also has two main components; inertial discs and the counterweight (Figure 11). Both of these are adjustable depending on the weight and height of the subject. The inertial discs are made from dense materials such as Corian and cultured marble. The counterweight is currently a container suspended to the end of chain. This specific design was chosen for the inertia system because it is easy to disassemble thus increasing portability. We chose to have the chain traveling over the subject's head because this decreased the interference between the subject and the chain.

### **Materials and Costs**

Shown in Table 2 is the cost of our prototype made from a combination of wood and plastic parts. Our device cannot contain ferrous materials so we had to perform an extensive search to find the adequate components. Most of the costs incurred for this design were from the plastic ball bearings, plastic sprockets and the polypropylene chain.

The relatively high cost is a result of the limited manufacturers of these components. The frame and base were constructed from standard construction materials such as wall studs and plywood. Along with the wood, the Corian and cultured marble disks were donated from a neighboring company.

**Table 2: Material Used in Design**

MATERIALS						
Quantity	Materials	Company	Part Number	Material	Cost/Unit	Price
3	Plastic Sprocket	SDP-SI	A 6M 7-Z5019	Acetal Resin, White	\$6.94	\$20.82
2	Plastic Ball Bearings	SDP-SI	A 7Z 5-G2010	Acetal/glass balls	\$18.59	\$37.18
2	Plastic Ball Bearings	SDP-SI	A 7Z 5-1306A	Acetal/glass balls	\$9.85	\$19.70
10	Plastic Chain	SDP-SI	A 6M 7-50PLP	Polypropylene	\$3.73	\$37.30
1	Plastic Disk	McMaster Carr	8582K22	Delrin	\$17.24	\$17.24
1	Plastic Rod	McMaster Carr	8701K45	UHMWPE	\$1.38	-----
1	Plastic Rod	McMaster Carr	8701K42	UHMWPE	\$1.26	-----
1	Plastic Dowel	McMaster Carr	8576K49	Fiberglass	\$10.34	-----
2	Plastic Nut	McMaster Carr	90059A031	UHMWPE	\$3.58	-----
1	Plastic Threaded Rod	McMaster Carr	98871A200	UHMWPE	\$10.71	-----
1	Standard 2"x4"x14'	-----	-----	Balsam	-----	-----
1	1-1/4" x 4' Wood Dowel	-----	-----	Oak	-----	-----
1	3/4"x18"x5'	-----	-----	Ply-wood	-----	-----
4	Inertial Disks	-----	-----	Corian	-----	-----
4	Inertial Disks	-----	-----	Cultured Marble	-----	-----
					<b>Total:</b>	\$132.24

## Manufacturing

We used a variety of machines to create our design: mill, lathe, drill press, band saw, and sander (Figures 12). The mill was used to make our hubbed disks and the pockets for the ball bearings in the inertia system assembly. A lathe was used to turn down Corian disks to ensure they would be concentric with the shaft about which they rotate. In order to make the cultured marble inertia disks, we utilized a drill press with a

4.5” hole saw. Lastly we used a band saw and sander to sculpt the wood to our specific design specifications.



**Figure 12: Manufacturing Pictures:** A variety of machines were used to make our device such as a band saw and drill press.

### **Future Work**

After the first prototype was constructed, we noticed some drawbacks in the device that previously went unnoticed. Thus, we would like to modify our existing design to accommodate more inertial disks and decrease the pitch diameter of the sprocket. This is necessary for the device to apply the appropriate inertia to subjects with stronger legs. In addition, we would like to place the rotating inertial shaft lower on the device, allowing us to design a new system for locking the frame components together. Furthermore, we are going to take our device into a motion capture lab, where we will use infrared cameras to test the accuracy of the motion. We will also determine if the motion is periodic and repeatable per our design constraints and develop a strategy to

train the subjects from the information. Modifications to the prototype may include using a metronome or some type of visual feedback system to aid the subject with the motion. Throughout the course of testing, we will determine if new methods need to be developed to prevent the chain from becoming slack. The dimensions of the current design are based off of previous measurements that need to be validated in the MRI. Ultimately, we will collect data from the subjects and verify the physiological representation of the force exerted on the hamstring in motion.

### **Ethics and Intellectual Property Issues**

Our device is not invasive however we must be aware of any opportunity to cause injury. Any chance to minimize risks associated with the operation of our device should be taken. We have incorporated the limit of 15% of the maximum voluntary contraction to prevent the subjects from fatigue which will also minimize the risk of re-injury. If the patient is at any moment in pain or feels discomfort, the motion may be stopped or the frequency of the motion may be reduced.

The intellectual property issues associated with this device include other teams and labs that have done similar testing. We must reference them accordingly for any aspect that may have been included in our design. While our design is intended for use in research, it is possible that this would be available to the public for use in diagnosing or gauging therapy and as a result, precautions to respect other patents as well as protect our own property will be taken.

## References and Works Consulted

- 1) Asakawa DS, Nayak KS, Blemker SS, Delp SL, Pauly JM, Nishimura DG, Gold GE. Real-time imaging of skeletal muscle velocity. *Journal of Magnetic Resonance Imaging*. 2003; 18:734-739.
- 2) Asakawa DS, Pappas GP, Blemker SS, Dracce JE, Delp SL. Cine phase-contrast magnetic resonance imaging as a tool for quantification of skeletal muscle motion. *Seminars in Musculoskeletal Radiology*. 2003; 7(4):287-295.
- 3) Asakawa DS, Blemker SS, Gold BE, Delp SL. In vivo motion of the rectus femoris muscle after tendon transfer surgery. *Journal of Biomechanics*. 2002; 35(8):1029-1037.
- 4) Asakawa DS, Pappas GP, Blemker SS, Drace JE, Delp SL. Cine phase-contrast magnetic resonance imaging as a tool for quantification of skeletal muscle motion. *Seminars in Musculoskeletal Radiology*. 2003; 7(4): 287-295.
- 5) Barance PJ, Williams GN, Novotny JE, Buchanan TS. A method for measurement of joint kinematics of 3-D geometric models with cine phase contrast magnetic resonance imaging data. *Journal of Biomechanical engineering*. 2005; 127:829-837.
- 6) Barrance P, Williams G, Sheehan FT, Buchanan TS. Measurement of tibiofemoral joint motion using CINE-Phase Contrast MRI.
- 7) Barrance P, Williams G, Sheehan FT, Buchanan TS. Measurement of tibiofemoral joint motion using CINE-Phase Contrast MRI.
- 8) Fellows RA, Hill NA, MacIntyre NJ, Harrison MM, Ellis RE, Wilson DR. Repeatability of a novel technique for in vivo measurement of three-dimensional patellar tracking using magnetic resonance imaging. *Journal of Magnetic Resonance Imaging*. 2005; 22: 145-153.
- 9) Komi PV. Stretch-shortening cycle: a powerful model to study normal and fatigued muscle. *Journal of Biomechanics*. 2000; 33:1197-1206.
- 10) Loudon, JK. Biomechanics of Gait and Running.  
<http://206.211.148.195/gettingfunctional/handouts/handout1.pdf>
- 11) Neu CP, Hull ML. Toward an MRI-based method to measure non-uniform cartilage deformation: an MRI-cyclic loading apparatus system and steady-state cyclic displacement of articular cartilage under compressive loading. *Journal of Biomechanical Engineering*. 2003; 125(2):180-188.

- 12)** Pappas GP, Asakawa DS, Delp SL, Zajac FE, Drace JE. Nonuniform shortening in the biceps brachii during elbow flexion. *Journal of Applied Physiology*. 2002; 92:2381-2389.
- 13)** Patel VV, Hall K, Ries M, Lotz J, Ozhinsky E, Lindsey C, Lu Y, Majumdar S. A three-dimensional MRI analysis of knee kinematics. *Journal of Orthopedic Research*. 2004; 22:283-292.
- 14)** Patel VV, Hall K, Ries M, Lindsey C, Ozhinsky E, Lu Y, Majumdar S. Magnetic resonance imaging of patellofemoral kinematics with weight-bearing. *Journal of Bone and Joint Surgery*. 2003; 85:2419-2424.
- 15)** Patel VV, Hall K, Ries M, Lindsey C, Ozhinsky E, Lu Y, Majumdar S. Magnetic resonance imaging of patellofemoral kinematics with weight-bearing. *Journal of Bone and Joint Surgery*. 2003; 85:2419-2424.
- 16)** Rebmann AJ, Rausch T, Shibanuma N, Sheehan FT. The precision of CINE-PC and Fast-PC sequences in measuring skeletal kinematics. *Proc. Intl. Soc. Mag. Reson. Med*. 2001; 9: 83.
- 17)** Rebmann AJ, Sheehan FT. Precise 3D skeletal kinematics using fast phase contrast magnetic resonance imaging. *Journal of Magnetic Resonance Imaging*. 2003; 17: 206-213.
- 18)** Sheehan FT, Drace JE. Quantitative MR measures of three-dimensional patellar kinematics as a research and diagnostic tool. *Medicine and Science in Sports and Exercise*. 1999; 31(10): 1339-??.
- 19)** Sheehan F, Zajac FE, Drace J. Imaging musculoskeletal function using dynamic MRI. *Rehabilitation R&D Center Progress Report*. 1996.
- 20)** Thelen DG, Chumanov ES, Sherry MA, Heiderscheit BC. Neuromusculoskeletal models provide insights into the mechanisms and rehabilitation of hamstring strains. *Exercise and Sports Science Reviews*. 2006; 34(3): 135-141.
- 21)** University of California, Los Angeles. *Human Locomotion Research Center*. 2004.
- 22)** Vedi V, Williams A, Tennant SJ, Spouse E, Hunt DM, Gedroyc WMW. Meniscal movement: an in vivo study using dynamic MRI. *British Editorial Society of Bone and Joint Surgery*. 1999; 81-B(1):37-41.

# Appendix

## Anthropometric Data

### ANTHROPOMETRIC PARAMETERS

most data taken from Plagenhoef S, Evans FG, Abdelnour T: Anatomical data for analyzing human motion, Res Q Exerc Sport 54:169, 1983. Data noted with \* is taken from Winter, DA: *Biomechanics of Human Movement* New York: John Wiley & Sons, 1978. Data noted with † is not taken from this reference, but is given as a rough approximation.

Segment Mass as Percentage of Total Body Mass		
Segment	Male	Female
Hand	0.65	0.5
Forearm	1.87	1.57
Upper arm	3.25	2.9
Foot	1.43	1.33
Shank (lower leg)	4.75	5.35
Shank and foot*	6.1	6.1
Thigh	10.5	11.75
Whole trunk	55.1	53.2
Head and neck	8.26	8.2

Location of the Segment Center of Mass as a Percentage of the Segment Length (measured from proximal or distal end of segment)					
Segment	Male		Female		
	Proximal	Distal	Proximal	Distal	
Hand	46.8	---	46.8	---	
Forearm	43.0	57.0	43.4	56.6	
Upper arm	43.6	56.4	45.8	54.2	
Foot	50.0	---	50.0	---	
Shank (lower leg)	43.4	56.6	41.9	58.1	
Shank and foot*	60.6	39.4	60.6	39.4	
Thigh	43.3	56.7	42.8	57.2	
Whole trunk <sup>a</sup>	63.0	37.0	56.9	43.1	
Head and neck <sup>b</sup>	55.0	45.0	55.0	45.0	

<sup>a</sup>Hip joint to shoulder joint = 100%

<sup>b</sup>Top of the head to 7th cervical = 100%

Radius of Gyration About Proximal Or Distal Segment End as a Percentage of Segment Length					
Segment	Male		Female		
	Proximal	Distal	Proximal	Distal	
Hand	54.9	---	54.9	---	
Forearm	52.6	64.7	53.0	64.3	
Upper arm	54.2	64.5	56.4	62.3	
Foot	69.0	---	69.0	---	
Shank (lower leg)	52.9	64.2	51.4	65.7	
Thigh	54.0	65.3	53.5	65.8	

Segment Length as a Percentage of Total Height		
Segment	Male	Female
Hand (to center of gravity)	5.75	5.75
Hand <sup>†</sup> (wrist to fingertips)	12.3	12.3
Forearm	15.7	16.0
Upper arm	17.2	17.3
Foot (to center of gravity)	4.25	4.25
Foot <sup>†</sup> (ankle to 1 <sup>st</sup> metatarsal head)	8.0	8.0
Shank (lower leg, knee to ankle)	24.7	25.0
Shank + foot (knee to sole of foot) <sup>†</sup>	28.2	28.2
Thigh	23.2	24.9
Trunk (hip to shoulder)	30.0	29.0
Head and neck (shoulder to head CM)	10.75	10.75
Shoulder to shoulder (gleno-hum)	24.5	20.0
Hip to hip	11.3	12.0

## Equations and Values for Extreme Anthropometric Limits

	EvaluatedValues		Design Variables
	Input Values		
		Male	Female
h	height of subject	1.905	1.499
m	mass of subject	115	40
T	Torque	50	5
r <sub>p</sub>	radius of pulley	0.0508	0.038608
r <sub>d</sub>	radius of disc	0.1524	0.15
l <sub>f</sub>	foot length	0.1524	0.11992
l <sub>s</sub>	shank length	0.470535	0.37475
l <sub>s&amp;f</sub>	shank and foot length	0.53721	0.422718
l <sub>f(45deg)</sub>	height of foot at 45 degrees	0.107763073	0.084796245
k <sub>foot</sub>	Radius of Gyration of Foot	0.105156	0.0827448
k <sub>shank</sub>	Radius of Gyration of Shank	0.248913015	0.1926215
r <sub>COM</sub>	radius of leg (knee to COM of shank and foot)	0.32554926	0.256167108
r <sub>COM(foot)/ankle</sub>	extra distance from ankle to COM of ankle	0.0762	0.05996
m <sub>s</sub>	mass of shank	5.4625	2.14
m <sub>f</sub>	mass of foot	1.6445	0.532
m <sub>s&amp;f</sub>	mass of shank and foot	7.015	2.44
I <sub>e</sub>	Inertia of Equivalent Mass [system]	9.724794931	0.900915425
I <sub>s</sub>	Inertia of Shank wrt Knee	0.338443876	0.07940051
I <sub>f</sub>	Inertia of Foot wrt Knee	0.509757085	0.104175967
I <sub>O</sub>	Inertia of Leg	0.848200962	0.183576477
θ <sub>max</sub>	Maximum Angle of Leg [radians]	0.839917089	0.922679055
θ <sub>min</sub>	Minimum Angle of Leg [radians]	0.201967952	0.201967952
θ <sub>O</sub>	Angle of Leg in "middle" position [radians]	0.52094252	0.562323503

$$\theta_o = \frac{\theta_{\max} - \theta_{\min}}{2} + \theta_{\min}$$

ω 2\*pi\*f 3.141592654 3.141592654

θ(t) position amplitude 1.041885041 1.124647007

$$\theta = \theta_o + \theta_o \sin \alpha t$$

ω(t) angular velocity amplitude 1.636589195 1.766591387

$$\dot{\theta} = \theta_o \omega \cos \omega t$$

α(t) angular acceleration amplitude 5.141496592 5.549910523

$$\ddot{\theta} = -\theta_o \omega^2 \sin \alpha t$$

cos(θ) Cosine of theta 0.867350475 0.846018612

sin(θ) Sine of theta 0.497697854 0.533153362

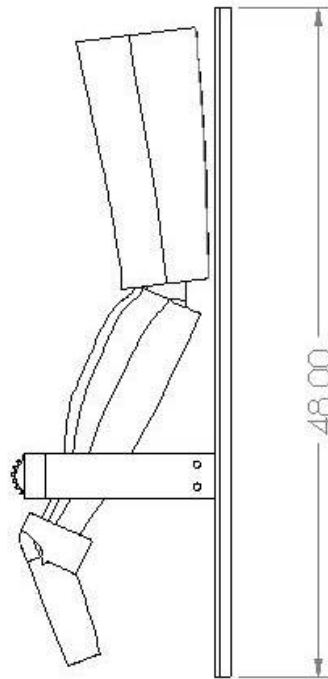
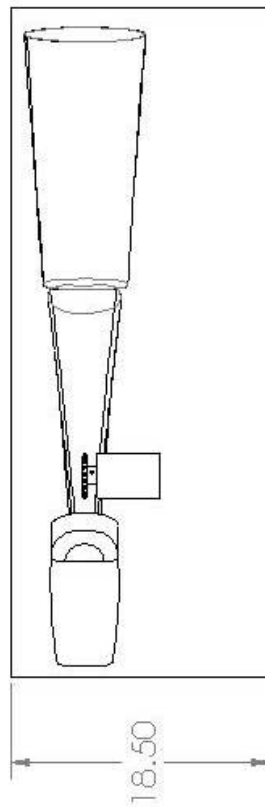
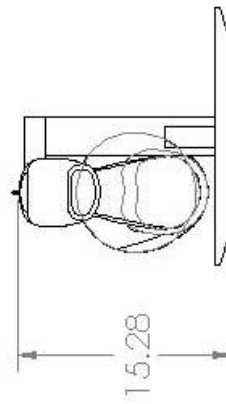
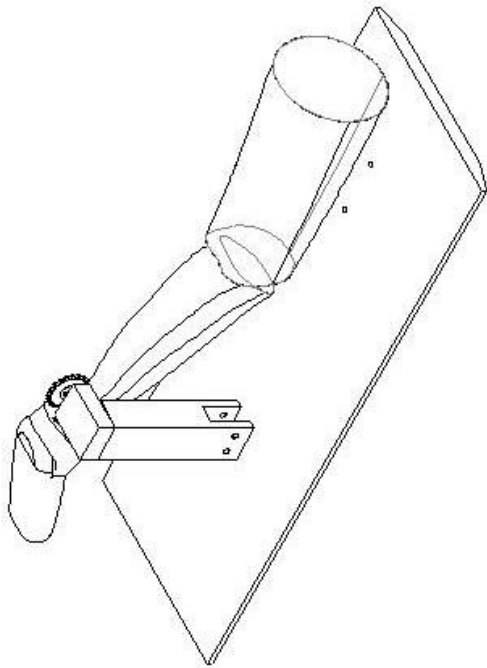
m<sub>l</sub> Mass of Load to Counter-Balance Leg  

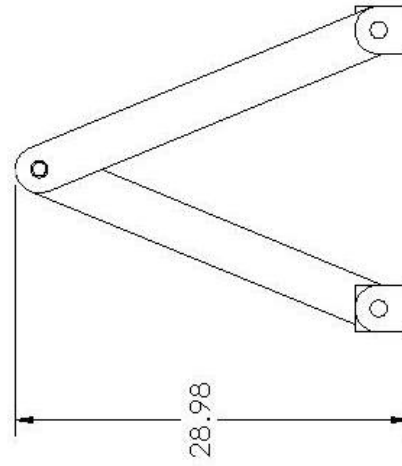
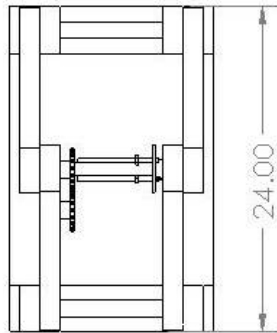
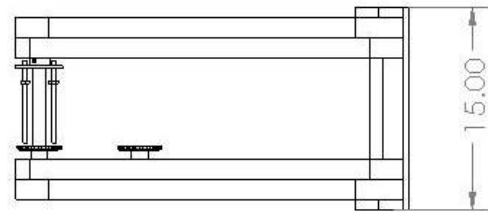
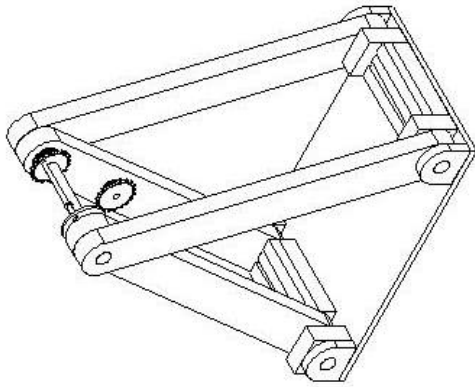
$$m_l = \frac{(m_{s\&f}) r_{COM} \cos \theta}{l_s (\cos \theta + \sin \theta)}$$
 - 1.023135242  
 2.401390687 -

I<sub>d</sub> Inertia of Disc  

$$I_d = \frac{(I_e - m_s l_s^2 - I_O) r_p^2}{l_s^2}$$
 - 0.004423863  
 0.07350518 -

## Dimensions of Design





## **Product Design Specifications**

### **An MR-Compatible Device for Imaging the Lower Extremity During Movement and Under Load**

**Team Members:** Sarajane Stevens, Arinne Lyman, Christopher Westphal, Eric Bader

**Client:** Professor Darryl Thelen

**Advisor:** Professor William Murphy

**Function:** MR imaging can provide clinicians and researchers valuable insights into the morphology of musculoskeletal structures. However, most current imaging techniques in use are static and do not provide direct measurements of biomechanical function. Recent breakthroughs in magnet strength, acquisition speed and processing of MR data have enabled imaging to be used to measure in-vivo muscle motion and joint kinematics during movement. These applications require the use of a non-magnetic device for loading or guiding the limb through a desired, repeatable movement. The goal of this design project is to develop and build such a device for use in the Radiology clinic of the UW Hospital. Our initial application is to use Cine-PC (Phase Contrast) imaging to measure in-vivo musculotendon motion of the hamstrings during a stretch-shortening cycle. Cine-PC requires multiple cycles of motion, necessitating that the device guide the limb through a repeatable motion at relatively low loads.

#### **Client requirements:**

- Provide repeatable, harmonic motion
- Same start and end points constrained by bore size
- Generate physiological load on hamstring
- Simulate swing phase of running
- Support thigh—limit movement
- Active movement by subject provides force
- Image near center of magnet
- Non-metallic, non-ferrous materials

#### **Design requirements:**

##### **1. Physical and Operational Characteristics**

a. *Performance requirements:* The device should fit the dimensions of a standard MRI machine and provide a physiological load to the hamstring under repeated, harmonic motion. The endpoints should be constrained so as to start and stop the motion in the same position.

- b. *Safety*: The load on the patient must not injure the limb under any conditions. The device must not contain metal due to effects of the strong magnet in the MRI.
- c. *Accuracy and Reliability*: Motion of the path should be accurate to  $\pm 1^\circ$  at the start and end point, and  $\pm 3^\circ$  at any point throughout the cycle. The same amount of force should be delivered during each motion within  $\pm 5\%$ .
- d. *Life in Service*: This is a research device that will be periodically used 2-3 times per week imaging 10-20 subjects at a time. The device may sit for a couple months between research dates. The device will be used for about three years.
- e. *Shelf Life*: Device will be stored in hospital storage cabinets. Shelf life should be about 5 years.
- f. *Operating Environment*: The device will be stored and used at room temperature in a hospital environment. It need not be sterile, but should be easily cleanable.
- g. *Ergonomics*: The force that the device applies to the patient must not exceed normal physiological loads for the individual. Device should also be easy to assemble and disassemble for technicians.
- h. *Size*: Size of the device is limited by the size of the MRI bore which is 60cm. Device should not take up unnecessary space around the MRI machine and not interfere with the technician's pathway to the machine.
- i. *Weight*: Device should weigh about 25lbs, adequate enough to transport from location to location. Device should also be able to be disassembled for easy transport.
- j. *Materials*: No metallic or ferrous materials can be used in our device. UW Hospital has a list of unacceptable MR materials we have already requested.
- k. *Aesthetics, Appearance, and Finish*: No special finishes are needed. Device should not be cumbersome to the patient.

## **2. Production Characteristics**

- a. *Quantity*: One prototype is requested at this time
- b. *Target Product Cost*: \$200

### 3. Miscellaneous

a. *Standards and Specifications*: The only standard is that the device cannot contain metallic or ferrous materials. The device also must not cause any harm to the patient.

b. *Customer*: The client would prefer to have a variable physiological force, so the use of a combination of force producers can be used.

c. *Patient-related concerns*: Device does not need to be sterilized. Should be accommodating to all patients, but some size restraints may exclude some patients.

d. *Competition*: There exist a number of devices that apply a load to the knee for imaging under MRI, however our device will be the first to mimic physiological loading during swing phase while taking dynamic images of the knee under this load.